Measuring the superconducting coherence length in thin films using a two-coil experiment

John Draskovic,[*] Thomas R. Lemberger, Brian Peters, and Fengyuan Yang

Department of Physics, The Ohio State University, Columbus, Ohio 43210, USA

Jaseung Ku and Alexey Bezryadin

Department of Physics, University of Illinois at Urbana-Champaign, Urbana, Illinois 61801, USA

Song Wang

Department of Physics, Stanford University, Stanford, California 94305, USA

We present measurements of the superconducting coherence length ξ in thin ($d \leqslant 100$-Å) films of MoGe and Nb using a combination of linear and nonlinear mutual inductance techniques. As the alternating current in the drive coil is increased at a fixed temperature, we see a crossover from linear to nonlinear coupling to the pickup coil, consistent with the unbinding of vortex-antivortex pairs as the peak pair momentum nears $\hbar/\xi$ and the unbinding barrier vanishes. We compare measurements of ξ performed by this mutual inductance technique to values determined from the films' upper critical fields, thereby confirming the applicability of a recent calculation of the upper limit on a vortex-free state in our experiment.

I. INTRODUCTION

The two-coil experiment is a long-established method for measuring the superfluid density $n_s \propto 1/\lambda^2$ in thin films,[1] where λ is the London penetration depth. A common geometry is a pair of coaxial coils located on opposite sides of the film sample. The drive coil is located closer to the film's surface and is energized with an alternating current. Meissner currents flow within the film to screen the small applied magnetic field from the drive coil. Coupling to the second (pickup) coil is measured as a function of temperature. Provided that the induced screening current in the film is far below its critical value, the order parameter is spatially uniform and the film can be described by a single complex conductivity. The imaginary part of this conductivity, deduced from the linear coupling between the coils, is used to calculate the superfluid density as a function of temperature.[2,3]

The present paper is preceded by those of Scharnhorst[4] and Claassen *et al.*[5] in which experimental critical currents were deduced from the onset of nonlinear (third-harmonic) response as the drive coil current was increased for metallic and cuprate films, respectively. Our approach expands this work in that we measure the fundamental response (amplitude and phase) over four decades of driving current, revealing heretofore unexamined features, such as the unbinding of vortex-antivortex (V-aV) pairs and hysteresis due to vortex pinning.

Using a simple model of our experiment, Lemberger and Draskovic[6] showed that milli-Gauss fields can sustain equilibrium V-aV pairs, assuming that there is no free-energy barrier to their unbinding. As such, all two-coil measurements, whether linear or nonlinear, are performed with the film in a metastable Meissner state governed by the unbinding barrier. Lemberger and Ahmed[7] calculated the upper limit of this metastable state as a function of the film's penetration depth. They found that

$$B_0^{\text{crit}} \approx \Phi_0/2R\xi \tag{1}$$

for films in the limit of long two-dimensional penetration depth $\Lambda \equiv 2\lambda^2/d \gg R$, where d is the film thickness and R is the radial position on the film where the applied perpendicular field changes sign. In the limit of short penetration depth $\Lambda \ll R$, they found

$$B_0^{\text{crit}} \approx \Phi_0/2\pi \Lambda\xi. \tag{2}$$

As a practical matter, our goal is to measure the coherence length in ultrathin cuprate films where determining ξ from the upper critical field B_{c2} is problematic. Our nonlinear measurements are easily performed at $T/T_c \ll 1$, and the vortex physics appears at tiny magnetic fields ($B_0 < 10$ G), where B_0 is the largest perpendicular field applied to the film, namely, the field applied at the center of the film.

II. EXPERIMENT

Thin films of amorphous molybdenum-germanium (*a*-MoGe) with thicknesses of 40, 50, 60, and 100 Å (measured by calibrated deposition) were rf sputtered onto 8×8-mm^2 SiO$_2$-capped silicon substrates with an average rate of 0.45 Å/s, giving T_c's in a range from 3 to 6 K. Nb films with T_c's in a range from 2 to 7 K were prepared on 15×15-mm^2 substrates at 1.5 Å/s. The thicknesses of the Nb films (19, 41, 54, and 62 Å) were determined by an empirical fit of $T_c(d)$ determined previously[8] for films of identical preparation. The Nb films received a cap layer of several hundred angstroms of Ge sputtered at 2 Å/s to prevent oxidation of the film between growth and characterization.

Our coils are wound from Nb-Ti wire with $T_c \approx 9$ K, higher than the highest-T_c films in this study. The applied perpendicular field $B_z(\rho)$ and in-plane vector potential $A_\phi(\rho)$ from the drive coil are displayed in Fig. 1. $R \approx 1.4$ mm is the radial distance at which B_z changes sign, a little more than double the coil radius. A commercial audio amplifier provided 10-kHz sinusoidal drive currents ranging from <50 μA to 1 A.
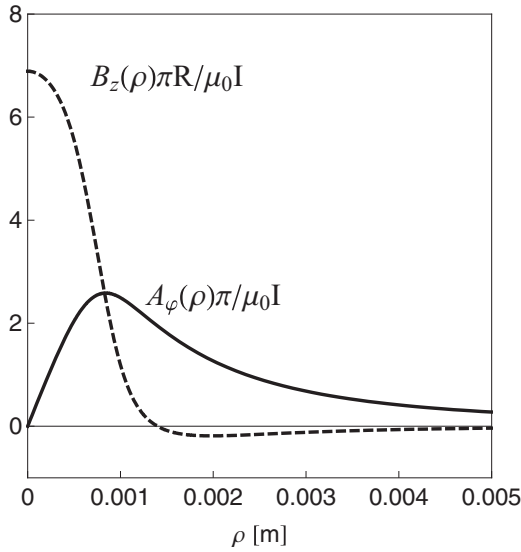
FIG. 1. Perpendicular magnetic field (dashed line) and the vector potential (solid line) produced by the experimental drive coil. The drive coil, radius of 660 μm, consists of 16 turns of Nb-Ti wire around a plastic form and is located 380 μm from the film surface.

Drive coil current and voltage across the pickup coil were measured by lock-in amplifiers.

Measurements were performed according to the following schedule for each film: The sample was cooled to 1.4 K in our two-coil cryostat. Nonlinear measurements were conducted at 1.4 K. Linear measurements were conducted as the two-coil cryostat warmed. The sample was then transferred to a physical property measurement system (PPMS®) (Quantum Design) and was cooled again to measure the resistance transition (the Nb films were cut down to fit the sample holder). High magnetic-field sweeps were performed at fixed low temperatures, and the sample was warmed again. Table I summarizes the measurements performed on the eight films.

A. Linear measurements

To determine the magnetic penetration depths, the alternating current in the drive coil was held well below the nonlinear crossover (i.e., $B_0 < 5$ mG), and the cryostat was allowed to

TABLE I. Measurements performed on four MoGe films and four Nb films. $T_{c,\rho}$ is the transition temperature as measured by four-terminal resistance. $T_{c,0}$ and $\Lambda(0) \equiv 2\lambda^2/d \propto 1/n_s(0)$ are from a dirty-limit BCS fit to the superfluid density data. $\xi_{Bc2}(0) \equiv \sqrt{\Phi_0/2\pi B_{c2}(0)}$.

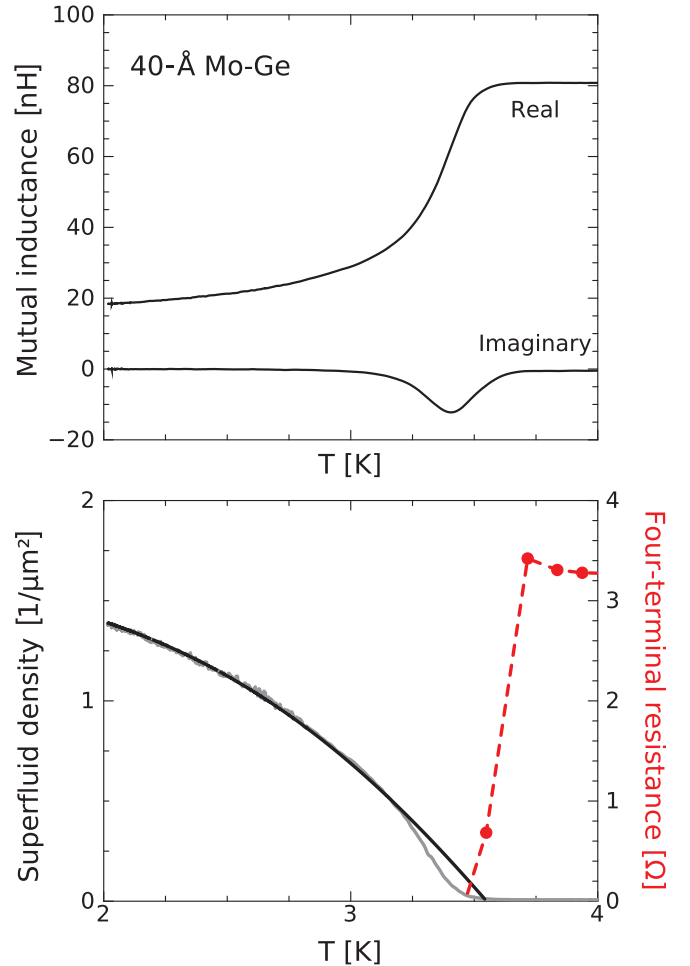|	d (Å)	$T_{c,\rho}$ (K)	$T_{c,0}$ (K)	$\Lambda(0)$ (μm)	B_{NL} (1.4 K) (G)	$\xi_{Bc2}(0)$ (Å)
MoGe	40	3.6	3.55	312	2.8	71
	60	4.9	5.00	133	7.2	69
	80	5.6	5.55	71	7.5	55
	100	5.3	5.46	68	8.3	56
Nb	19	2.6	2.22	505	0.72	92
	41	4.5	4.45	65	2.4	105
	54	5.8	5.50	16	8.6	107
	62	6.4	6.00	10	14.4	110

FIG. 2. (Color online) (Top) Complex mutual inductance as a function of temperature in the linear regime for a typical MoGe film. The upper curve is the real part of the mutual inductance $M = V_p/\omega I_d$, where V_p is the out-of-phase component of the pickup coil voltage and I_d is the drive coil current. The lower curve is the imaginary part. (Bottom) Superfluid density and four-terminal resistance as a function of temperature for the same film. The black line is a dirty-limit BCS fit to the data (gray).

warm up. Superfluid density data were fit to the BCS dirty limit per Refs. 8 and 9 with a gap parameter of $\Delta(0)/k_B T_c = 1.9$. Typical data for mutual inductance, corresponding superfluid densities $\lambda^{-2}(T)$, and four-terminal resistances for *a*-MoGe and Nb films are shown in Figs. 2 and 3. Note that the superfluid density diminishes below the mean field $T_{c,0}$ for these films. This is also evident in the appearance of nonzero resistance below the mean-field transition. We attribute this to currents in the film exceeding the critical current near the transition. We believe that this deviation in superfluid would diminish if suitably small drive/excitation currents had been used. We are confident that our experimental values of $1/\Lambda(T \to 0)$ are accurate to $\pm 10\%$. $1/\Lambda$ is measured directly, so uncertainty in film thickness is irrelevant.[2,3]

B. Nonlinear measurements

Nonlinear measurements were conducted with the experimental probe submerged in a LHe bath at the lowest
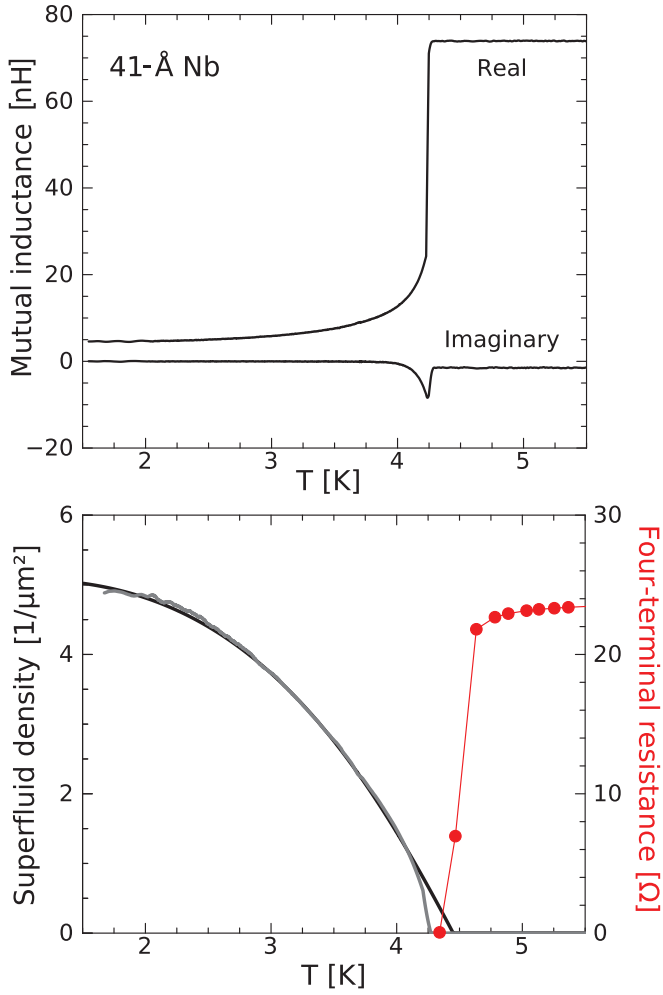
FIG. 3. (Color online) (Top) Complex mutual inductance as a function of temperature in the linear regime for a typical Nb film. (Bottom) Superfluid density and four-terminal resistance as a function of temperature for the same film.

FIG. 4. (Color online) Scaled complex mutual inductance of four MoGe films and four Nb films (M_0 is the mutual inductance when the film is in the normal state) as a function of the applied magnetic-field amplitude at the center of the film B_0, scaled by the applied field where the mutual inductance has reached half of its normal-state value B_{NL} (solid curves). The dotted curves are the absolute value of imaginary mutual inductance normalized to its peak value.

temperature achievable by pumping on the bath, approximately 1.4 K. We feel that the combination of superconducting coils and immersion in LHe is sufficient to nullify the coil heating concerns raised by Refs. 4 and 5 where nonsuperconducting coils were used. Samples were cooled to 1.4 K in liquid helium with the drive coil deenergized. The drive coil current was increased to produce the mutual inductance curves of Fig. 4.

The linear-response regime, clearly indicated by a field-independent value of the real part of mutual inductance, crosses over to a regime where the mutual inductance rises monotonically toward its normal-state value M_0. We characterize this effect by the value of B_0 at which the mutual inductance has risen halfway to its normal-state value, denoting this field as B_{NL}. The similarity of the scaled curves demonstrates the consistency of this effect across films of different thicknesses and compositions. We note that these curves are only very weakly dependent on frequency in the range of 1–20 kHz where our electronics are linear and postpone a thorough exploration of the frequency domain.
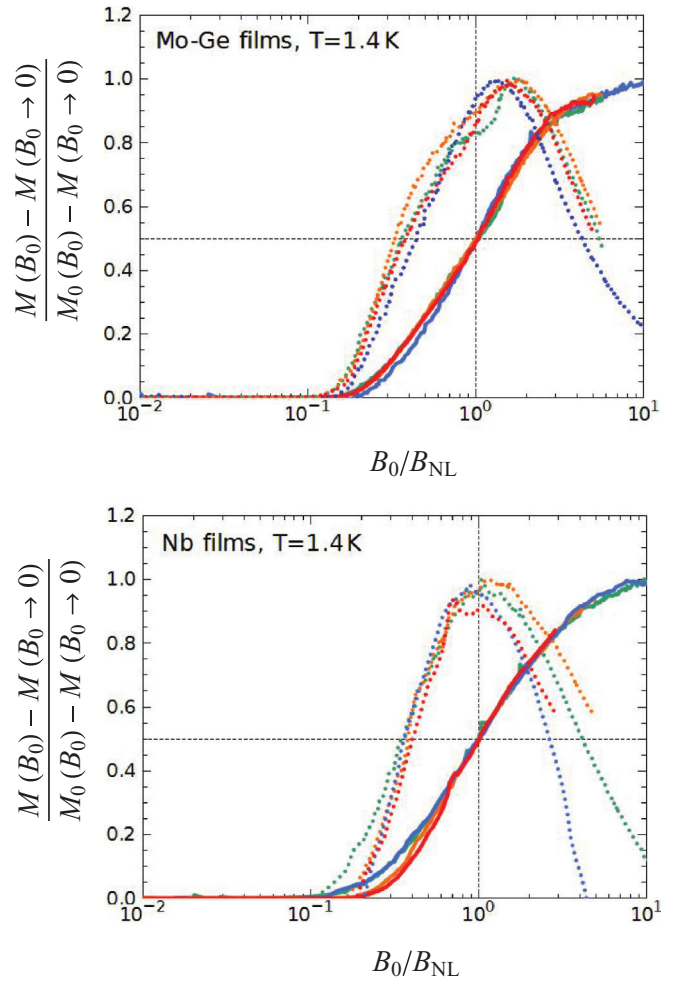
C. High-field measurements

We measured perpendicular upper critical fields $B_{c2}(T)$ from resistive transitions R_{sheet} vs B in fields up to 14 T in a Quantum Design PPMS® as shown in Figs. 5 and 6. Samples were wired in a Van der Pauw configuration. To determine $\xi(0)$, $B_{c2}(T)$ was extrapolated to zero temperature by fitting to the dirty-limit Abrikosov-Gor'kov form.[10] We found that determining $B_{c2}(T)$ by a four-terminal resistance value of 90% of the normal-state value gave $B_{c2}(0)$ values consistent with textbook data.[11,12] Uncertainty in ξ_{Bc2} is set by the width of the resistive transitions (*see insets to Figs. 5 and 6*). The broadest transitions produce an uncertainty of ±25% in B_{c2}, but given the inverse-square relationship between B_{c2} and ξ, the error in ξ is halved.

Dirty-limit BCS theory is applicable if the mean-free path l is less than the coherence length. In amorphous MoGe, $l < 10$ Å (a few interatomic spacings) for thick films.[13] Since our films are thicker than 10 Å, surface scattering should not be important. The dirty limit gives $\xi \propto \sqrt{\hbar v_f l / \pi \Delta(0)}$, so for
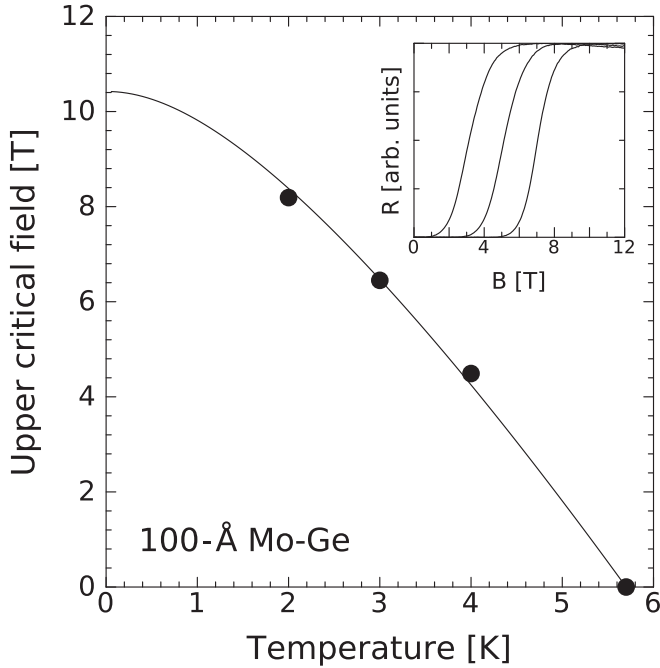
FIG. 5. Upper critical field B_{c2} as a function of temperature for a MoGe film. $B_{c2}(T)$ is determined by the measured resistance reaching 90% of its normal-state value for constant temperature data as well as constant field data for $B = 0$. The fit is the Abrikosov-Gor'kov curve.

constant l and Fermi velocity, we expect

$$\xi = \xi^{T_c=7.3 \text{ K}} \sqrt{\frac{7.3 \text{ K}}{T_c}} \quad \text{(MoGe films)}, \quad (3)$$

which fits ξ_{Bc2} well with $\xi_{Bc2}^{T_c=7.3 \text{ K}} = 65$ Å for MoGe.

In thin Nb, the mean-free path *is* limited by surface scattering:[8] $l \approx d/4$. Since $T_c \propto d$ for low-T_c films, we expect

$$\xi = \xi^{T_c=8.5 \text{ K}} \approx \text{Const.} \quad \text{(Nb films)}. \quad (4)$$
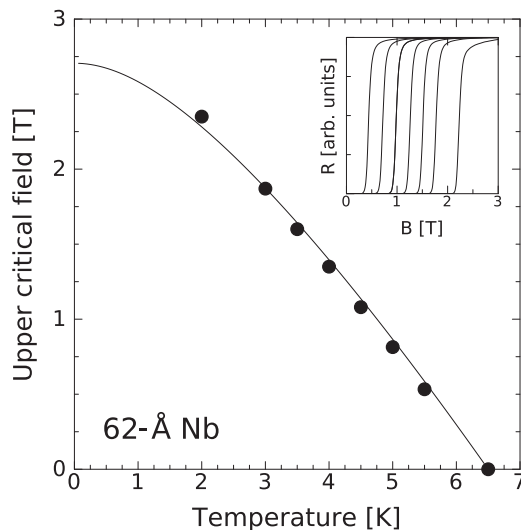

FIG. 6. Upper critical field B_{c2} as a function of temperature for a Nb film.

The mean of our B_{c2}-derived values for Nb is 103 Å $\pm 8\%$—constant with respect to our experimental uncertainty.

III. DISCUSSION

The similarity of the curves in Fig. 4 from film to film and between Nb and *a*-MoGe argues that the basic physics is largely the same in all films, regardless of differences in disorder, vortex pinning details, etc. A simple critical state model of the vortex behavior based on a "puddle" of vortices forming at the center of the film under each cycle of the driving field captures the qualitative features of the experimental data, namely, a rise in the real mutual inductance coincident with a peak in the imaginary mutual inductance signal. The imaginary mutual inductance is a result of hysteresis in the areal densities of vortices and antivortices, a feature that is not seen unless pinning is included in the model. The model calculations, details of which are the subject of a forthcoming paper, indicate that the real mutual inductance rises with a near-vertical slope and reaches 50% of the normal-state value within a factor of 2 of the field of first vortex-antivortex unbinding at zero temperature. The peak in the calculated imaginary mutual inductance occurs simultaneously. Given the plausibility of V-aV pairs unbinding thermally in our finite-temperature experiment, we take B_{NL} to correspond to the bulk unbinding of vortex-antivortex pairs in the data rather than the field at which the signal first deviates from linearity, approximately $B_{\text{NL}}/5$.

In Fig. 7, the B_{NL} values of Table I are fitted to the model of Ref. 7 [Eqs. (1) and (2)] using the functional forms of Eqs. (3) and (4) with $\xi^{T_c=7.3 \text{ K}}$ and $\xi^{T_c=8.5 \text{ K}}$ as free parameters for MoGe and Nb, respectively. This amounts to a qualitative test of the model, and the fit is excellent. The model gives quantitative agreement as well: The fit parameters used in Fig. 7 give factor-of-2 agreement with the B_{c2}-determined values.
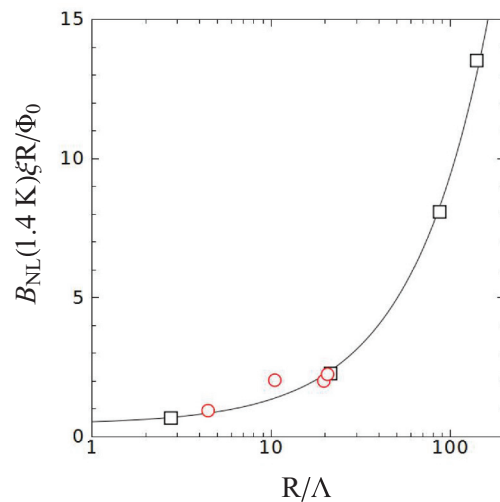

FIG. 7. (Color online) Normalized B_{NL} measurements plotted as a function of dimensionless superfluid density R/Λ and fitted to the single-ring model of Lemberger and Ahmed:[7] $y \approx 0.45 + 0.09x$. ξ for each material is the only fitting parameter as per Eqs. (3) and (4). The fit gives $\xi^{T_c=7.3 \text{ K}} = 33$ Å for MoGe films (red circles) and $\xi^{T_c=8.5 \text{ K}} = 135$ Å for Nb films (black squares).

IV. SUMMARY

We have measured the complete crossover of linear-to-nonlinear two-coil response for two well-understood dirty-limit BCS superconductors. We have empirically identified the applied driving magnetic field associated with vortex-antivortex pairs unbinding *en masse* in the films, informed by a microscopic model which includes flux pinning. Our data on eight films fit well to Lemberger and Ahmed's recent calculation of the upper bound of the vortex-free state as a function of superfluid density,[7] and we are able to extract values of the superconducting coherence length from these data in quantitative agreement with values measured from the films' upper critical fields.

*draskovic.1@osu.edu

[1] A. Fiory, A. Hebard, P. Mankiewich, and R. Howard, Appl. Phys. Lett. **52**, 2165 (1988).

[2] S. J. Turneaure, A. A. Pesetski, and T. R. Lemberger, J. Appl. Phys. **83**, 4334 (1998).

[3] S. J. Turneaure, E. R. Ulm, and T. R. Lemberger, J. Appl. Phys. **79**, 4221 (1996).

[4] P. Scharnhorst, Phys. Rev. B **1**, 4295 (1970).

[5] J. Claassen, M. Reeves, and R. Soulen, Rev. Sci. Instrum. **62**, 996 (1990).

[6] T. R. Lemberger and J. Draskovic, Phys. Rev. B **87**, 064503 (2013).

[7] T. R. Lemberger and A. Ahmed, Phys. Rev. B **87**, 214505 (2013).

[8] T. R. Lemberger, I. Hetel, J. W. Knepper, and F. Y. Yang, Phys. Rev. B **76**, 094515 (2007).

[9] S. J. Turneaure, T. R. Lemberger, and J. M. Graybeal, Phys. Rev. Lett. **84**, 987 (2000).

[10] E. Helfand and N. Werthamer, Phys. Rev. **147**, 288 (1966).

[11] A. Bezryadin, *Superconductivity in Nanowires* (Wiley-VCH, Weinheim, Germany, 2013), Appendix A.

[12] A. Engel, A. Semenov, H. Hübers, K. Il'in, and M. Siegel, in *New Frontiers in Superconductivity Research*, edited by B. Martins (Nova Science, New York, 2006).

[13] J. M. Graybeal and M. R. Beasley, Phys. Rev. B **29**, 4167 (1984).